

**Synthesis of Tantalum Doped
Sodium-Potassium Niobate System**
By
Solid state Reaction Technique

A THESIS SUBMITTED IN PARTIAL FULFILMENT
OF THE REQUIREMENTS FOR THE DEGREE OF

Bachelor of Technology
In
Ceramic Engineering
By

Durjodhan Barla
Roll – 10508017

Under the Guidance of
Prof. R.Mazumder



Department of Ceramic Engineering
National Institute of Technology ,Rourkela
2005 – 2009



CERTIFICATE

This is to certify that the thesis entitled “***Synthesis of Tantalum doped Sodium- Potassium Niobate system by solid state reaction technique***” submitted by Mr. **Durjodhan Barla** in partial fulfillment of the requirements for the award of Bachelor of Technology Degree in **Ceramic Engineering** at **National Institute of Technology, Rourkela** (Deemed University) is an authentic work carried out by him under my supervision and guidance.

To the best of my knowledge, the matter embodied in the thesis has not been submitted to any other University / Institute for the award of any Degree or Diploma.

Date:- 13-05-2009

Prof. R. Mazumder
Dept. of Ceramic Engg
National Institute of Technology
Rourkela – 769008

ACKNOWLEDGEMENTS

On the submission of my thesis report of “Synthesis of tantalum doped Sodium-Potassium Niobate system by solid state reaction technique”, I would like to convey my gratitude & sincere thanks to my supervisor Prof R.Mazumder, Department of Ceramic Engineering for his constant motivation and support during the course of my work in the last one year. I truly appreciate and value his esteemed guidance and encouragement from the beginning to the end of this thesis. I am indebted to him for having helped me shape the problem and providing insights towards the solution.

I want to thank all my teachers and post graduate seniors for providing a solid background for our studies and research thereafter. They have been great sources of inspiration to me and I thank them from the bottom of my heart.

Above all, I would like to thank all my friends whose direct and indirect support helped me completing my project in time. This thesis would have been impossible without their perpetual moral support.

Contents

- 1. Abstract**
- 2. General Introduction**
 - 2.1 Introduction
 - 2.2 objective of this thesis
- 3. Experimental Work**
 - 3.1 procedure
 - 3.2 calculations
 - 3.3 choice of fuel
- 4. Results and Discussions**
 - 4.1 XRD Analysis
- 5. References**

1. Abstract

Due to the toxicity of lead, there is an urgent need to develop lead-free alternatives to replace the currently dominant lead-based piezoelectrics such as lead zirconate titanate (PZT). (Na_{0.5}K_{0.5})NbO₃ (NKN)-based piezoelectrics are promising because of their relatively high Curie temperatures and piezoelectric coefficients among the non-lead piezoelectrics. However, it is difficult to sinter.

Sodium potassium niobate [(Na_{0.5}K_{0.5})NbO₃ or NKN], the main material system on which the research of this thesis work is centered. The challenges for lead-free materials to replace lead-based families and the approaches to improve the piezoelectric performance of lead-free systems by adding dopants to the system.

2. General Introduction

Only the materials that have no center of symmetry in their crystalline structures possess piezoelectricity. For the direct piezoelectric effect, when a mechanical stress T is applied to the piezoelectric material, the charge generated is proportional to the force. The general equations that relate the electric and elastic variables can be written as:

$$D = dT + \epsilon TE \quad (2.1)$$

where D is dielectric displacement (electric flux density per unit area) and d is called piezoelectric charge constant (or “piezoelectric constant” in short) that has an unit of coulombs/Newton.

It can be understood as induced polarization per unit stress. ϵT is the permittivity while the stress remains constant. For the converse piezoelectric effect, the induced strain S can be expressed in terms of the applied electric field E .

$$S = sET + dE \quad (2.2)$$

In this case d has a unit of meters/Volt. sE is the elastic compliance and remains constant under the electric field. Although this unit of d is different from what is used for the direct effect, the coefficient d has a numerically identical value to what is shown in equations (2.1) and (2.2). It can be understood as induced strain per unit electric field.

In practice, because piezoelectric materials are anisotropic, the response to an applied electric field or the mechanical force in different directions can be very different. Therefore, d is actually a tensor and many other physical properties of piezoelectric materials have two subscripts (1, 2 or 3) that indicate the directions of two related quantities. By convention, the subscript 3 denotes the poling direction of the material. 1 and 2 are two arbitrarily chosen orthogonal axes in the plane normal to 3. For piezoelectric charge constant d_{ij} , the first subscript denotes the direction

of polarization generated in the material or the direction of the applied electric field. The second subscript denotes the direction of the applied stress or the induced strain, respectively. For example, d_{33} represents the induced polarization in direction 3 per unit stress applied along direction 3. d_{31} represents the induced strain along direction 1 (perpendicular to direction 3) per unit electric field applied along direction 3.

The electrical-mechanical energy conversion efficiency of a piezoelectric element can be indicated by electromechanical coupling factor k . The square of k measures the fraction of the mechanical energy delivered into the piezoelectric element converted to electrical energy (or vice versa), namely

$$k^2 = (\text{input mechanical energy converted into electrical energy}) / (\text{input mechanical energy}) \quad (2.3)$$

$$\text{or } k^2 = (\text{input electrical energy converted into mechanical energy}) / (\text{input electrical energy}) \quad (2.4)$$

In practice, because the conversion between the two forms of energy is never complete, k^2 is always smaller than 1 (so is k). The actual expression of k is dictated by the shape of the piezoelectric element. For example, for a thin piezoelectric ceramic disc, the planar coupling factor, k^2 , is used to express radial coupling, i. e. the coupling between an electric field parallel to the direction along which the ceramic is polarized and mechanical response that causes radial vibrations, relative to the poling direction. k_p is related to the piezoelectric constant d and the dielectric constant ϵ_{33} :

$$k_p = d_{31} / (\epsilon_{33} / s_{11} + s_{12})^{1/2} \quad (2.5)$$

There is a group of piezoelectrics called ferroelectric materials that exhibit spontaneous polarization, namely, polarization in the absence of an electric field. This spontaneous polarization is a result of the positioning of the cations and anions within the unit cell of the material when the temperature is below a characteristic temperature (called Curie temperature or T_c). The direction of the spontaneous polarization can be switched by an external electric field.

POLING:

Ferroelectric materials commonly display very high dielectric constant at low frequencies. Many of them have fairly good piezoelectric properties after the spontaneous polarization within the unit cells are aligned by an application of an electric field. Ceramics are polycrystalline. In other words, a ceramic can be thought of as an agglomeration of small crystals (or grains) fitted together in a random manner in terms of the crystalline orientation within each individual grain. At a temperature below the Curie temperature, a ferroelectric ceramic lengthens along the direction of the polar axis so dipoles form in individual grains. But because of the random orientation of grains resulting in the cancelation of polarization from each grain, the net polarization of the ceramic is therefore zero even though the individual grains may be strongly piezoelectric. Thus, in order to polarize a ferroelectric ceramic so it can be piezoelectric, an electric field is required to switch the polar axis to the direction nearest to that of the field and allowed by the crystalline symmetry. This process is called “poling”. After poling, a ferroelectric ceramic can resemble a piezoelectric single crystal because it now has a net polarization.

Although a ferroelectric ceramic can “resemble” by lining up their polar axes to an extent through poling, its piezoelectric performance is always much lower than that of its single crystal counterpart. But because ferroelectric ceramics are normally much easier to fabricate than single crystals and the fabrication and their processing are also more economical, they are widely used in most of piezoelectric applications where extremely high piezoelectricity is not required.

Perovskite ferroelectrics

Perovskite piezoelectrics are of the great importance among all the piezoelectric ceramics because most of the piezoelectric materials used today belong to this family. This structure has a general formula ABO_3 and may be described as a simple cubic unit cell with the corners occupied by a large cation (“A”, such as Pb, Ba, Ca, K, Na, etc.), a smaller cation (“B”, such as Ti, Nb, Mg, Zr, etc.) and oxygens in the face centers, as shown in Figure 2.1.

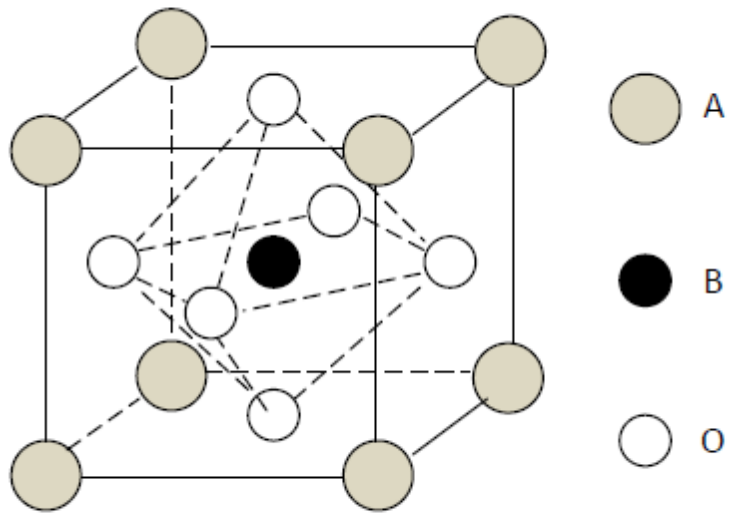


Figure 2.1 Schematic of the perovskite structure (ABO₃)

This structure can also be visualized as corner-linked oxygen octahedra with a small cation sitting in the center (B) of the octahedron and a large cation (A) filling the dodecahedral hole in between the oxygen octahedral. In practice, any structure similar to what is shown in Figure 2.1 but slightly distorted can be considered a perovskite. Also, in some cases, there can be multiple cations in the A site or B site. For instance, PZT has both Zr and Ti at the B site; one of the major lead-free piezoelectric candidates, which is also the main material system this thesis study is focused on, sodium potassium niobate (NKN), has both Na and K at the A site.

Lead-based piezoelectric materials

Most of the used piezoelectric materials used today are lead-based. The PZT family mentioned above is the most common one. PZT dominates the field of piezoelectrics because strong piezoelectric effects are shown in this material, especially at the compositions near the morphotropic phase boundary [Pb(Zr_{0.52}Ti_{0.48})O₃]. The morphotropic phase boundary of PZT is almost vertical in the phase diagram, as shown in Figure 2.2¹⁰, which maintains the excellent piezoelectric properties across a wide temperature change.

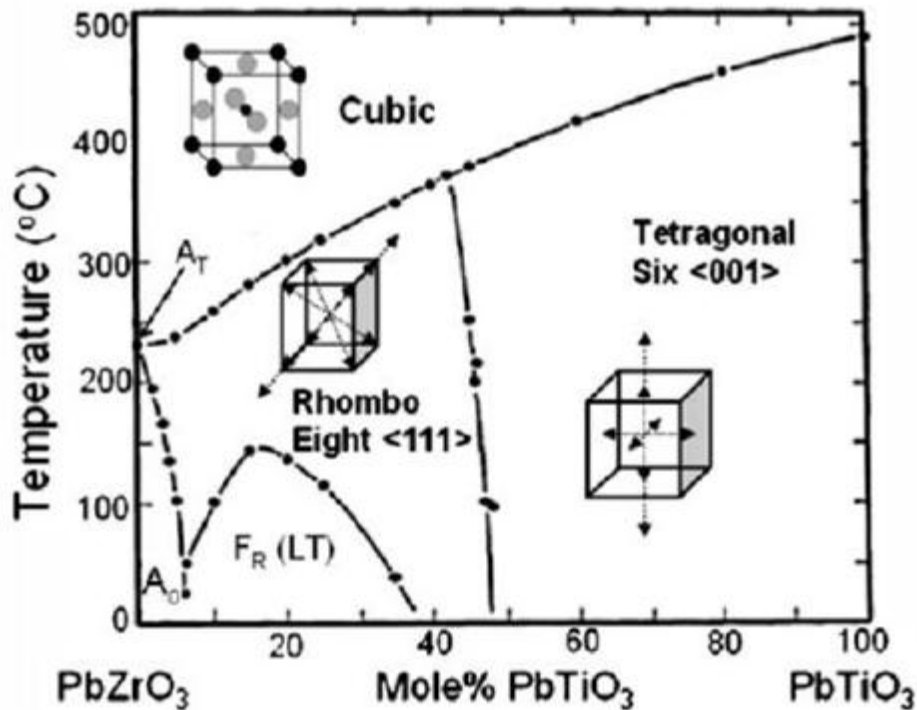


Figure 2.2 Phase diagram of lead zirconate titanate¹⁰

Besides PZT, some newer generations of lead-based piezoelectrics that exhibit exceptional piezoelectric properties were also created by combining PbTiO₃ (PT) with some lead-based ferroelectrics such as Pb(Zn_{1/3}Nb_{2/3})O₃ (PZN) and Pb(Mg_{1/3}Nb_{2/3})O₃ (PMN) to form solid solutions. The d_{33} of the <001>-cut PZN-PT single crystal with the near-MPB composition (10%PT) is as high as 2500 pC/N¹¹ and that of PMN-PT crystals with MPB compositions (35%PT) is 1500 pC/N.¹² Moreover, these materials also show very high dielectric constants at room temperature owing to the broadening of the permittivity peak around the Curie temperature.

Current lead-free piezoelectric materials:

As introduced in Chapter 1, the quest for lead-free piezoelectric alternatives has been increasing around the globe. Among all the lead-free piezoelectric materials, two classes have

drawn the most attention: bismuth layer structured ferroelectrics (BLSF) and perovskite structured ferroelectrics. A typical structure of BLSF¹³ is shown in Figure 2.3. The structure consists of perovskite layers and $(\text{Bi}_2\text{O}_2)_2^+$ layers that separate the perovskite layers periodically. This class of compounds normally can be described by the formula: $(\text{Bi}_2\text{O}_2)_2^+ (\text{M}_{m-1}\text{RmO}_{3m+1})_2^-$, e.g., $\text{Bi}_4\text{Ti}_3\text{O}_{12}$ and $\text{Bi}_4\text{BaTi}_4\text{O}_{15}$. The crystal structure is composed of pseudo-perovskite blocks $(\text{M}_{m-1}\text{RmO}_{3m+1})_2^-$ interleaved with $(\text{Bi}_2\text{O}_2)_2^+$ layers. The m in the formula is the number of perovskite units within each perovskite layer. The layer structure makes the grains in polycrystalline BLSF having plate-like morphology. BLSF usually have high Curie temperatures ($600^\circ\text{C}\sim 900^\circ\text{C}$),^{14,15} much higher than those of the lead-based materials ($200^\circ\text{C}\sim 400^\circ\text{C}$), making BLSF good candidates for applications at high temperatures. Nevertheless, the drawback of BLSF is as evident as their advantage. Due to the anisotropic nature of their structures, the switching of the spontaneous polarization within the materials during poling is limited within a two-dimensional plane^{16,17} (the ab plane shown in Figure 2.3), resulting in the low piezoelectric properties in BLSF. The d_{33} of these materials are normally lower than 20 pC/N, which is one order of magnitude lower than those of lead-based piezoelectrics.

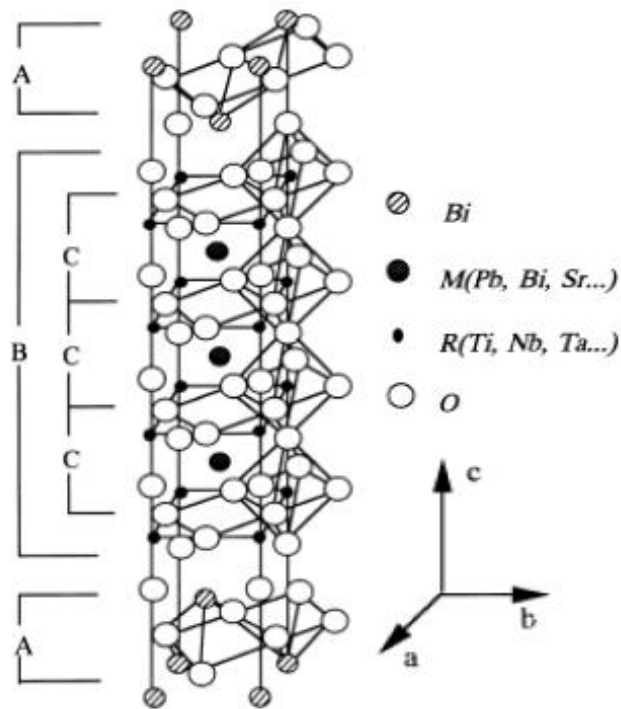


Figure 2.3 Bismuth layer structure¹³

In contrast, perovskite lead-free piezoelectric ceramics are of more importance because most members of this family possess good piezoelectric properties with BLSF. Barium titanate (BaTiO_3) is a typical example. Polycrystalline BaTiO_3 has dielectric constants of a few thousand and piezoelectric coefficients close to 200 pC/N .¹⁸ But the Curie temperature of BaTiO_3 is too low (120°C) for many applications. Two systems of this family, $(\text{Bi}_{1/2}\text{Na}_{1/2})\text{TiO}_3$ (BNT) and $(\text{Na}_{0.5}\text{K}_{0.5})\text{NbO}_3$ (NKN), have drawn a great deal of attention in recent years. $(\text{Bi}_{1/2}\text{Na}_{1/2})\text{TiO}_3$ shows large remnant polarization ($38 \text{ } \mu\text{C}/\text{cm}^2$). But it has a large coercive field ($73 \text{ kV}/\text{cm}$)¹⁹ and a ferroelectric-to-antiferroelectric phase transition at around 200°C . On the other hand, sodium potassium niobate, $\text{Na}_{0.5}\text{K}_{0.5}\text{NbO}_3$, is a good candidate because it has a fairly high Curie temperature (420°C). However, it's difficult to obtain fully dense $\text{Na}_{0.5}\text{K}_{0.5}\text{NbO}_3$ ceramics by ordinary sintering. Cold isostatic pressing (CIP) or hot-pressing is required to form $\text{Na}_{0.5}\text{K}_{0.5}\text{NbO}_3$ green compacts.²⁰⁻²³ It's been reported that hot-pressed $\text{Na}_{0.5}\text{K}_{0.5}\text{NbO}_3$ possesses high remnant polarization ($33 \text{ } \mu\text{C}/\text{cm}^2$), large longitudinal piezoelectric coefficient ($d_{33}=160 \text{ pC}/\text{N}$) and high planar coupling factor (0.45).²⁴ Saito et al. has

successfully textured a $\text{Na}_{0.5}\text{K}_{0.5}\text{NbO}_3$ -based material, LF4 [or $(\text{K}_{0.44}\text{Na}_{0.52}\text{Li}_{0.04})(\text{Nb}_{0.86}\text{Ta}_{0.10}\text{Sb}_{0.04})\text{O}_3$], and achieved the best piezoelectric coefficients ($d_{33}=416$ pC/N and $d_{31}=-152$ pC/N) of all the lead-free systems.²⁵ Some novel sintering aids ($\text{K}_4\text{CuNb}_8\text{O}_{23}$ 26,27 and $\text{K}_5.4\text{CuTa}_{10}\text{O}_{29}$ 28,29) have been developed to improve the sintering of $\text{Na}_{0.5}\text{K}_{0.5}\text{NbO}_3$. The microstructures were demonstrated to be much denser than those of NKN sintered without them.³⁰⁻³² But in those studies, CIP was still used to obtain the green compacts.

The comparisons of the electrical properties between current major systems and PZT are listed below.

Table 2.1: Electrical property comparisons between current major lead-free systems and PZT

	BLSF	Perovskite structured ferroelectrics			
	$\text{Bi}_4\text{Ti}_3\text{O}_{12}$	BaTiO_3	$(\text{Bi}_{1/2}\text{Na}_{1/2})\text{TiO}_3$	$(\text{Na}_{0.5}\text{K}_{0.5})\text{NbO}_3$	PZT
Curie temperature (°C)	683	120	320	420	300~400
d_{33} (pC/N)	<10	190	120~200	100~416	200~500
d_{31} (pC/N)	----	-78	-7.5	-30~-152	-130
Dielectric constant (at 1 kHz)	100~200	1500~6000	~1700	200~500	1000~4000

Figure 2.4(a) and (b) explicitly summarize the dielectric permittivity, piezoelectric coefficients as functions of Curie temperature for the current lead-free piezoelectrics in contrast to those of the PZT.³⁴ In practice, although piezoelectric performance evidently is the ultimate criteria to judge how good a piezoelectric is, a high Curie temperature is also strongly desired in order to provide a wide temperature range of operation and ensure the stability of the material performance. As shown in these two figures, one may notice that an empirical phenomenon is

that high piezoelectric coefficient and dielectric permittivity normally comes at the price of lowering the Curie temperature. $\text{Na}_0.5\text{K}_0.5\text{NbO}_3$ -based materials present a clear-cut advantage in possessing high piezoelectric performance while maintaining high Curie temperature. In Figure 2.4, it is also quite evident that the overall level of the piezoelectric performance of lead-free ceramics currently is still below that of PZT.

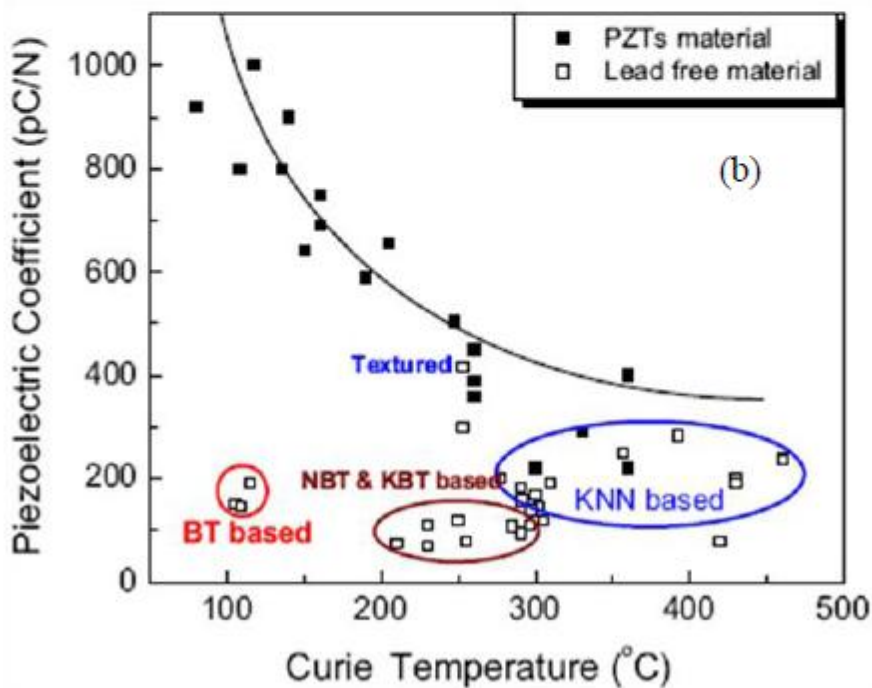
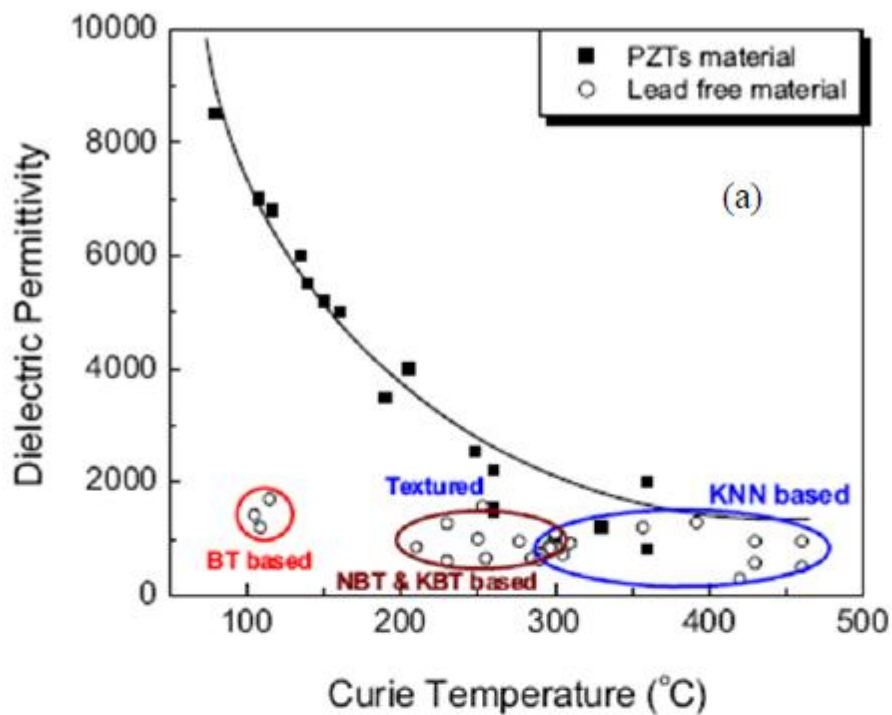


Figure 2.4 Property comparisons between PZT materials and lead-free materials: (a) dielectric permittivity as a function of Curie temperature; (b) piezoelectric coefficient as a function of temperature.³⁴

Current approaches to improve piezoelectrics:

Apparently, the piezoelectric properties of most the major lead-free systems mentioned above are lower than those of the PZT family. Various methods have been developed to improve the piezoelectric properties of piezoelectrics.

Construct solid solutions near morphotropic phase boundaries :

Morphotropic phase boundary (MPB) of a solid solution is an intrinsic region of a phase diagram where two or more different phases coexist. In many lead-based systems, it has been shown that the solid solutions of piezoelectric materials usually show the maximums of their piezoelectric properties (piezoelectric coefficients and electromechanical coupling factors) as well as dielectric constants at the compositions near the MPBs. For example, the piezoelectric coefficients of PZT with compositions near the MPB ($\text{Pb}(\text{Zr}_{0.52}\text{Ti}_{0.48})\text{O}_3$) are showed in Figure 2.5

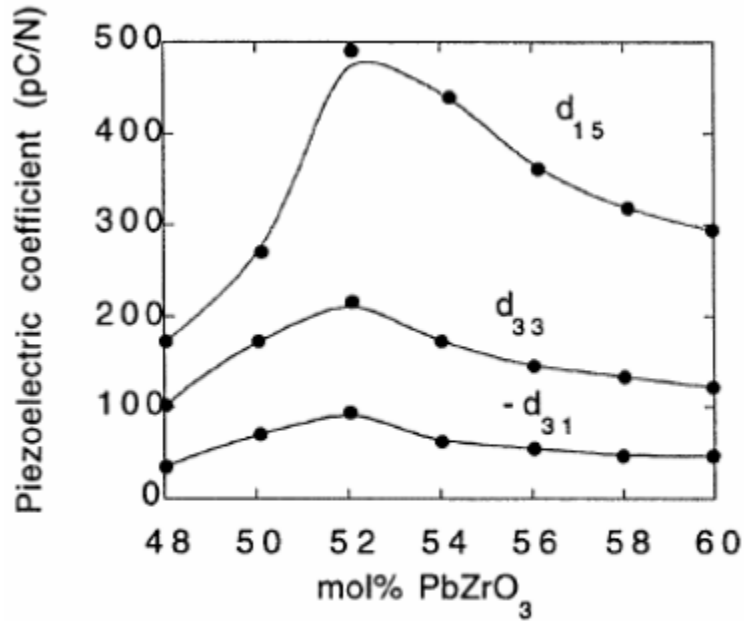


Figure 2.5 Variation of room temperature piezoelectric coefficients of PZT near the MPB.

The reason that these properties show the maximum at the MPB can be explained from a statistical point of view regarding the polar axis switching during the poling process of the materials. When a piezoelectric ceramics is poled, the different polar axes within the grains are forced to switch toward the directions that are allowed by crystallographic symmetry. Given a particular crystallographic symmetry, there are always a fixed number of equivalent polar axes which the dipoles can switch from. The numbers of polar axes of ferroelectrics with different phases are shown in Figure 2.6

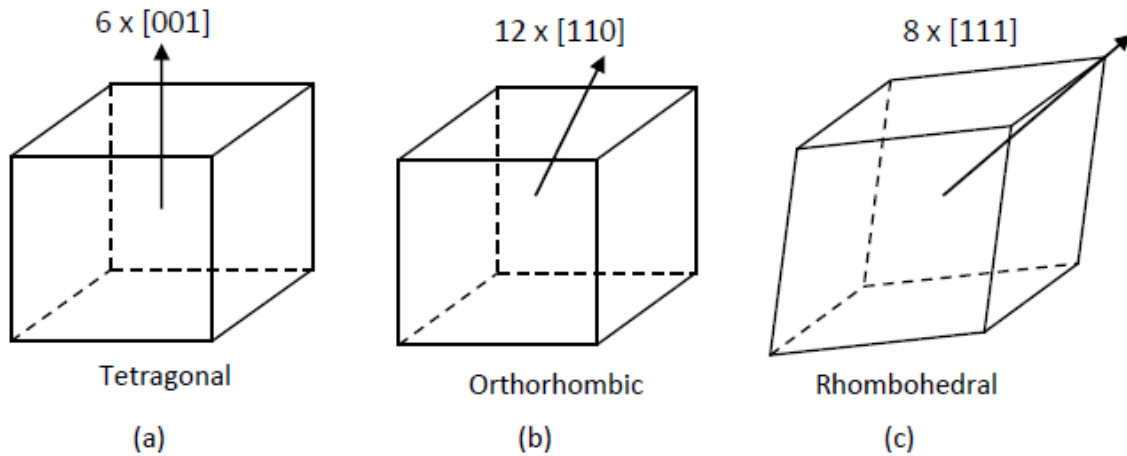


Figure 2.6 Numbers of equivalent polar axes of ferroelectrics with different phases: (a) six [001] directions in tetragonal; (b) twelve [110] directions in orthorhombic; (c) eight [111] directions in rhombohedral.

For instance, on the Zr-rich side of the MPB, the crystal symmetry of PZT is tetragonal, with 6 equivalent [001] directions as polar axes. On the Ti-rich side of the MPB, PZT is rhombohedral, with 8 equivalent [111] directions as polar axes. But at the MPB, two different phases coexist, so the switching of the polar axes in the material under a poling field now has 14 available directions. With a larger number of allowable polar directions, the maximum deviation of the polar axis of a grain from the average polar direction becomes smaller, so that the lowering of the net polarization in the whole polycrystalline specimen becomes less. In other words, MPB combines the allowable switching directions of polar axes of different phases so as to make the alignment of dipoles in grains become easier. As a result, the piezoelectric properties of the ferroelectrics are enhanced. A number of other piezoelectric materials have improved their piezoelectric performance by utilizing this method, such as $(1-x)\text{Pb}(\text{Mg}_{1/3}\text{Nb}_{2/3})\text{O}_3-x\text{PbTiO}_3$ (PMN-PT)^{35,36}, $(1-x)\text{Pb}(\text{Zn}_{1/3}\text{Nb}_{2/3})\text{O}_3-x\text{PbTiO}_3$ (PZN-PT)¹¹, $(\text{Bi}_{0.5}\text{Na}_{0.5})\text{TiO}_3\text{-BaTiO}_3$ (BNBT)^{37,38}.

2.1 Introduction

Sodium potassium niobate-based material systems :

The major drawback of current lead-free piezoelectrics is that their piezoelectric performance is still far lower than that of the dominating PZT family. Most of the efforts to achieve the piezoelectric properties close to those of PZT are made in perovskite ferroelectrics. Among these materials, sodium potassium niobate, $\text{Na}_{0.5}\text{K}_{0.5}\text{NbO}_3$ (abbreviated as NKN hereinafter), is a good candidate to replace PZT family because of its high Curie temperature and good piezoelectric properties. NKN is a solid solution of NaNbO_3 and KNbO_3 . The phase diagram of the KNbO_3 - NaNbO_3 system is given in Figure 2.13. There are three morphotropic phase boundaries observed in the phase diagram, located at around 52.5 mol%, 67.5 mol% and 82.5 mol% NaNbO_3 (marked by the dash lines in Figure 2.13), separating two different orthorhombic phases, respectively. In 1959, the dielectric and piezoelectric properties of $(1-x)\text{KNbO}_3$ - $x\text{NaNbO}_3$ were reported. It was found that the piezoelectric properties of $(1-x)\text{KNbO}_3$ - $x\text{NaNbO}_3$ present much less variation with composition than the PZT system. Around the MPB at 50 mol% NaNbO_3 , namely, $\text{Na}_{0.5}\text{K}_{0.5}\text{NbO}_3$, piezoelectric performance maximum ($d_{33}=80$ pC/N, $k_p=0.36$) was found. Therefore, intensive research effort has been focused on the $(1-x)\text{KNbO}_3$ - $x\text{NaNbO}_3$ materials around this composition of those three MPBs.

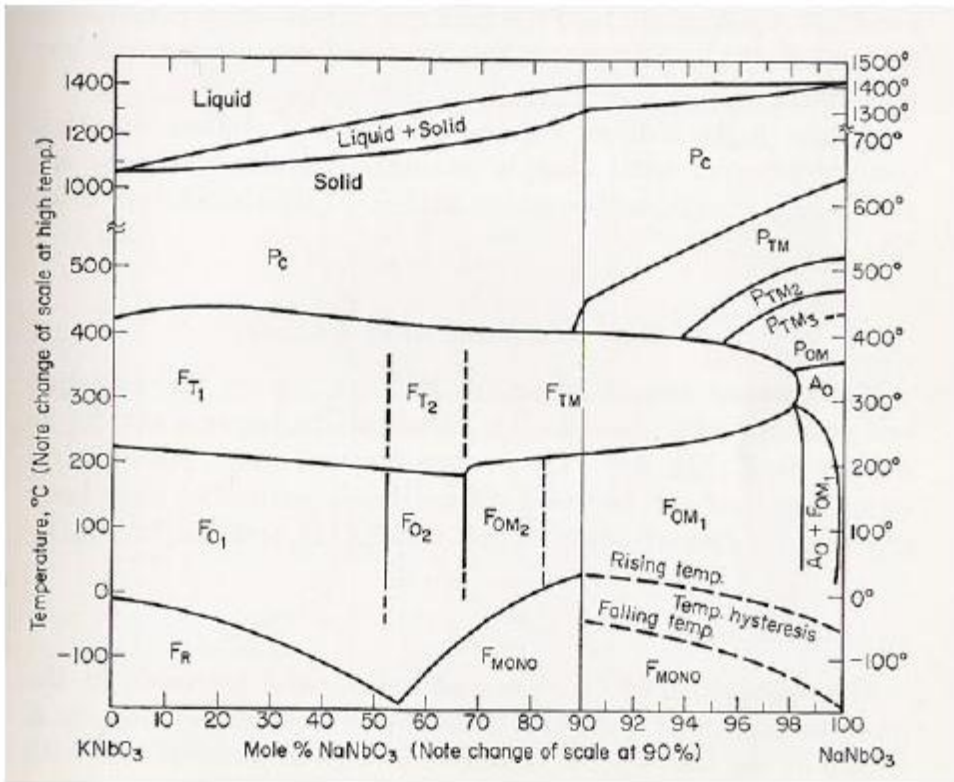


Figure 2.13 Phase diagram of KNbO_3 – NaNbO_3 solid solution.¹⁰

Problem in undoped NKN system:

A major problem of undoped NKN is that it is fairly difficult to sinter in air using the conventional uniaxial pressing technique due to the high volatility of the potassium component and the high reactivity with moisture. However, atmospheric firing is strongly desired for industrial production of ceramic. To improve the sintering of this material, various techniques were used. It was reported in 1962 that hot pressing greatly increased the sintered density from 4.25 g/cm³ to 4.46 g/cm³ and the d_{33} of this material was improved to 160 pC/N.²⁴ In recent years, approaches of using sintering aids were exploited. Several copper-based sintering aids have been developed for $\text{Na}_{0.5}\text{K}_{0.5}\text{NbO}_3$, such as CuO ^{57,58}, $\text{K}_4\text{CuNb}_8\text{O}_{23}$ (KCN)^{26,27} and $\text{K}_{5.4}\text{Cu}_{1.3}\text{Ta}_{10}\text{O}_{29}$ (KCT)^{28,29,59}. The microstructures shown in the SEM photographs are much

denser than those of NKN sintered without these sintering aids. 30-32 However, CIP was still used to obtain the green compacts in those studies and the dielectric and piezoelectric properties did not show improvements despite of the increase in sintered density of the ceramic.

To effectively increase the piezoelectric performance of $\text{Na}_0.5\text{K}_0.5\text{NbO}_3$, a few other materials have been used to form perovskite solid solutions with this system and create morphotropic phase boundaries to seek piezoelectric property enhancement at the MPBs. By far, the NKN-based solid solution systems reported are: NKN-SrTiO₃⁶⁰⁻⁶², NKN-(Bi_{0.5}K_{0.5})TiO₃⁶³, NKN-BaTiO₃^{64, 65}, NKN-LiTaO₃⁶⁶⁻⁶⁸, NKN-LiNbO₃⁶⁹⁻⁷³ and NKN-LiSbO₃⁷⁴⁻⁷⁶. The lead-free material with the best piezoelectric coefficients (reaching the level of those of PZT) has been obtained from a NKN-Li-TaSb system by Saito. However, to obtain the desired properties, a set of complex processing techniques are required, such as TGG which involves the fabrication of the template, tape casting and stacking tapes to make green compact.

In summary, the piezoelectric and dielectric properties reported for all the current NKN-based bulk materials are listed below in Table 2.2. As can be seen in Table 2.2, of all the current non-textured NKN-based materials, the NKN modified by combination of Li and Sb gives the best piezoelectric performance while maintaining high Curie temperature. In order to further engineer this system so as to exert its potential, the individual effect of Li and Sb on NKN needed to be comprehensively understood. Guo et al. has found that the maximum of piezoelectric properties of this system at 5-6 mol.% Li was a consequence of a MPB, the introduction of lithium actually resulted in a monotonic increase in the Curie temperature regardless of the piezoelectric maximum. However, the effect of Sb on the structure and the piezoelectric properties of Li-modified NKN remained unclear. Therefore, to fill in this void of knowledge, one of the specific objectives of this thesis study was to investigate the effect of varying the antimony concentration alone on the crystalline structure, piezoelectric and dielectric properties of NKN-LiNbO₃ with an MPB composition (5.5%).

Although doping, grain size control, texturing and solid solutions with near-MPB compositions are the main techniques to improve the piezoelectric properties of piezoelectric materials, the electric-field enhancement of piezoelectric response found in freestanding PMN-PT films suggests a new approach to significantly improve the piezoelectric performance of

piezoelectric materials. It was also of great interest to explore the possibility of translating this technique onto a lead-free system.

	ϵ/ϵ_0	$\tan\delta$	d_{33} (pC/N)	k_p	T_c (°C)
NKN	290	0.04	80	0.35	420
NKN (hot pressed)	420	0.035	160	0.46	420
NKN-Li-Ta-Sb (LF4T)*	1570	---	416	0.61	253
NKN-LiTaO ₃ (5%)	570	0.04	200	0.36	430
NKN-LiNbO ₃ (5%)	---	---	230	0.44	460
NKN-SrTiO ₃ (5%)	950	---	200	0.37	277
NKN-(Bi _{0.5} K _{0.5})TiO ₃ (3%)	850	0.04	192	0.45	370
NKN-BaTiO ₃ (2%)	1000	0.04	104	0.295	358
NKN-LiSbO ₃ (5%)	1288	0.019	283	0.50	392

Table 2.2 Dielectric and piezoelectric properties of current NKN-based lead-free systems

2.2 Objective of this thesis:

The main objective is to produce BiFeO₃ which must have the following characteristics :

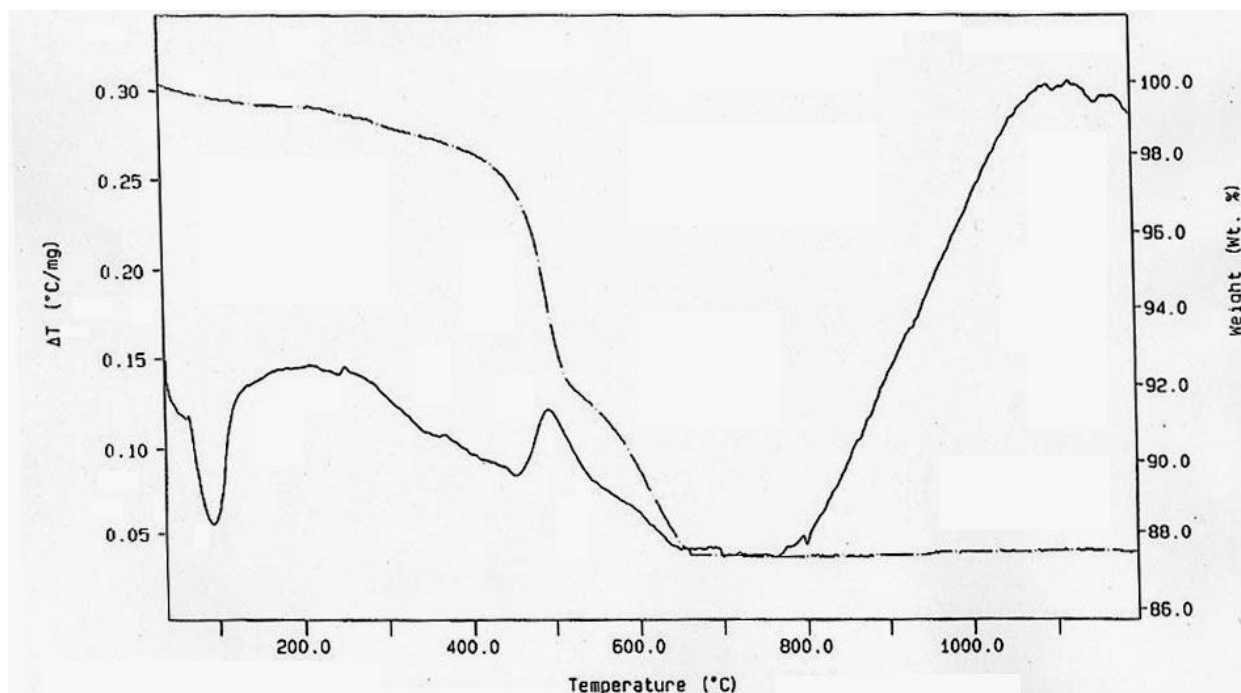
- I. Synthesizing phase pure material,
- II. Achieving lowest sintering temperature
- III. Comparing XRD peaks of NKN with tantalum doped NKN system
- IV. XRD analysis of NKN-Ta with variation of tantalum oxide

Chapter 3

Experimental Work

3.1 Solid state reaction Route

One of the most widely used and useful method of preparation of NKN is the solid state synthesis route. Samples were prepared by conventionally mixed oxide with the reagent grade of Starting materials of Na_2CO_3 , K_2CO_3 , Nb_2O_5 and Ta_2O_5 . The use of two different powders with carbonate origin requires extra care to be taken against humidity .TGA shows that Powder lose weight upto 120°C . Which is equivalent to the water absorbed. Therefore, In order to obtain stoichiometric material composition all powders were separately dried In an oven at 150°C for 24 hrs. prior to mixing. Then stoichiometric amounts of starting powder were weighed and transferred to an agate motar .Then grinding is done using Propan-2-ol medium for 24 hrs.After grinding, mixture were calcined at various calcinations conditions in an Aluminium crucible,i.e temperatures ranging from 850°C to 900°C ,dwell time ranging from 2 to 3 hrs.XRD was done for the calcined powder .



3.2 Batch Calculation:

For 5 gms of $\text{Na}_{0.5} \text{K}_{0.5} \text{Nb}_2\text{O}_3$, we require

Na_2CO_3 - 0.77 gms

K_2CO_3 - 1.0047gms

Nb_2O_5 - 3.864 gms

For 3 gms of $(\text{K}_{0.44}\text{Na}_{0.52}\text{Li}_{0.04})(\text{Nb}_{0.86}\text{Ta}_{0.10}\text{Sb}_{0.04})\text{O}_3$, we require

Na_2CO_3 -0.4585 gms

K_2CO_3 -0.5059 gms

Nb_2O_5 -1.9018 gms

Ta_2O_5 -0.3676 gms

LiCO_3 -0.0245 gms

Sb_2O_5 -0.1076 gms

For 3 gms of $(\text{K}_{0.5}\text{Na}_{0.5})(\text{Nb}_{1-x}\text{Ta}_x)$

When $x=5\%$

Na_2CO_3 -0.4507gms

K_2CO_3 -0.5877 gms

Nb_2O_5 -2.1478 gms

Ta_2O_5 -0.1879 gms

When x= 10%

Na_2CO_3 -0.4397gms

K_2CO_3 -0.5734 gms

Nb_2O_5 -1.9848 gms

Ta_2O_5 -0.3666 gms

When x= 15%

Na_2CO_3 -0.4293gms

K_2CO_3 -0.5598 gms

Nb_2O_5 -1.8304. gms

Ta_2O_5 -0.5369 gms

When x= 20%

Na_2CO_3 -0.4193gms

K_2CO_3 -0.5468 gms

Nb_2O_5 -1.6827. gms

Ta_2O_5 -0.6993 gms

When x= 25%

Na_2CO_3 -0.4098gms

K_2CO_3 -0.5344 gms

Nb_2O_5 -1.5417. gms

Ta_2O_5 -0.8543 gms

When x=30%

Na_2CO_3 -0.4007gms

K_2CO_3 -0.5225 gms

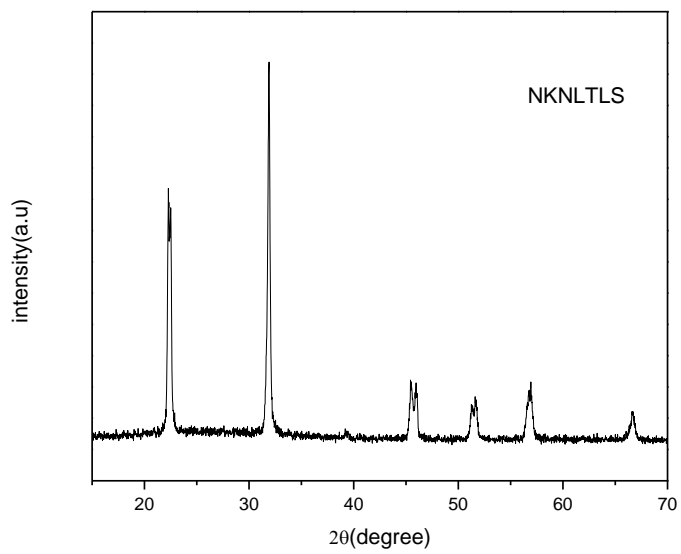
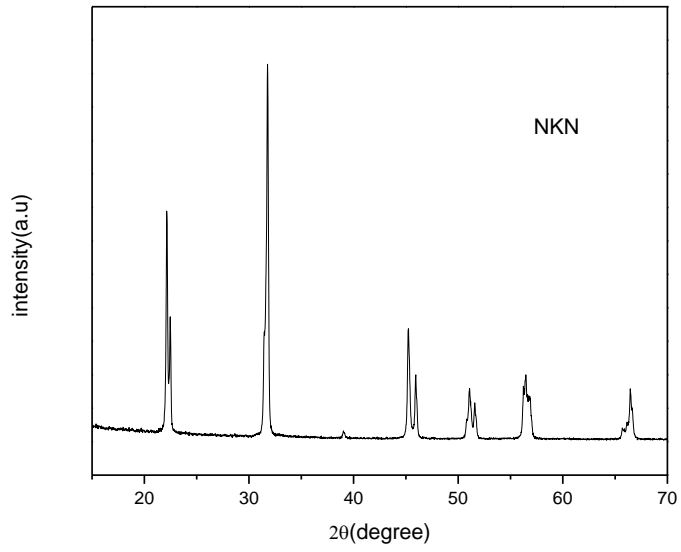
Nb₂O₅ -1.4070. gms

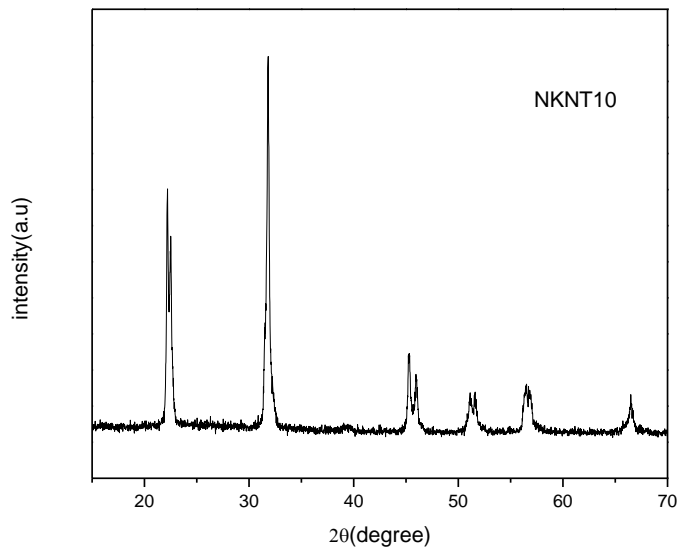
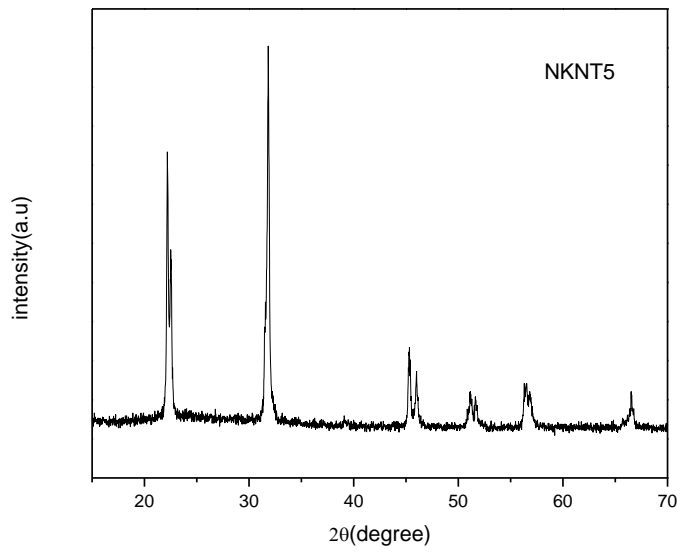
Ta₂O₅ -1.0024 gms

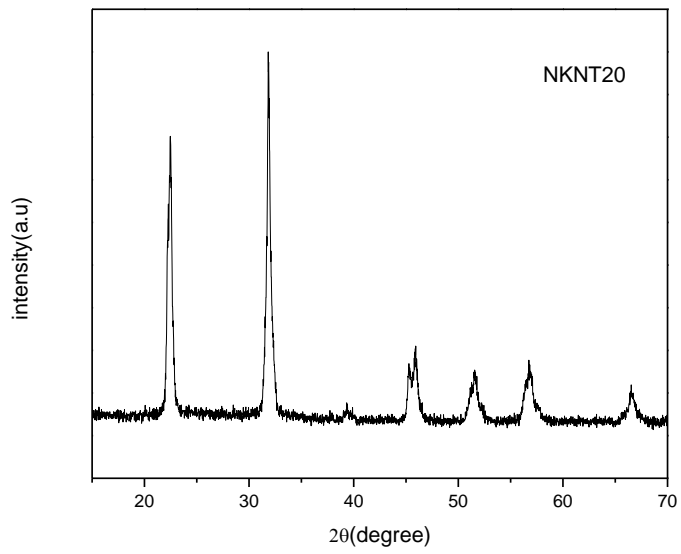
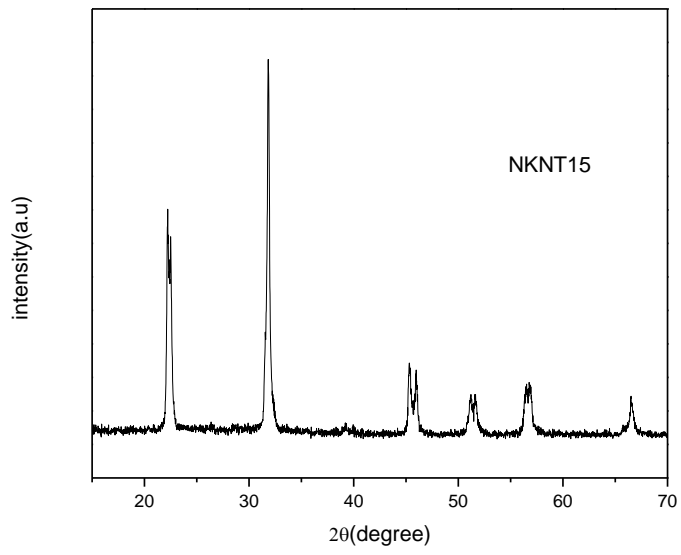
Chapter 4

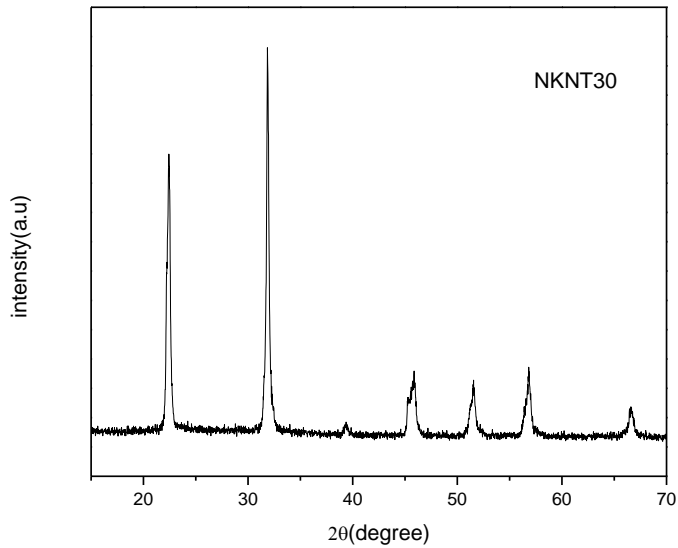
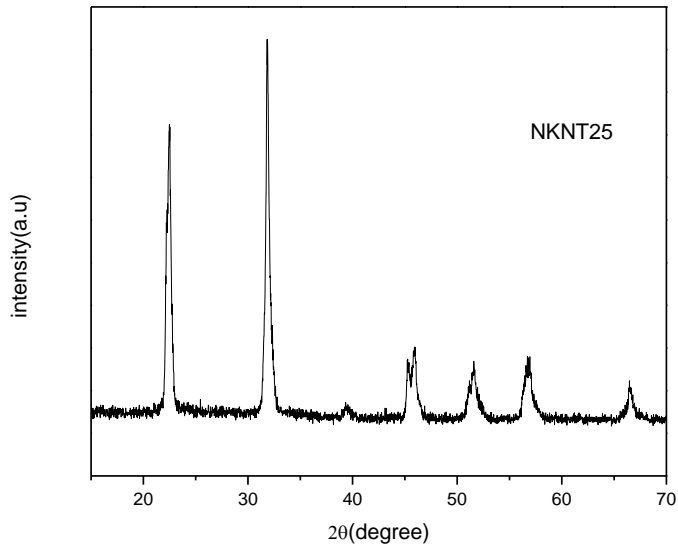
Results and Discussions

4.1 XRD Analysis









The XRD of the different samples was done and behavior was studied. From the above XRD graphs it is clear that peaks are slightly shifted due to phase transformation. The intensity of the peaks decreases with increase in tantanum oxide addition. Properties are enhanced due to formation of morphotropic phase boundary (MPB) .

References

1. B. Jaffe, W. R. Cook, and H. Jaffe, *Piezoelectric Ceramics* (Academic Press Limited, London, 1971).
2. J. Kuwata, K. Uchino, and S. Nomura, *Japanese Journal of Applied Physics* **21**, 1298-1302 (1982).
3. P. Seung-Eek and T. R. Shrout, *Ultrasonics, Ferroelectrics and Frequency Control*, IEEE Transactions on **44**, 1140-1147 (1997)
4. M. Miyayama and I.-S. Yi, *Ceramics International* **26**, 529-533 (2000).
5. T. Takenaka and K. Sakata, *Japanese Journal of Applied Physics* **19**, 31-39
6. Z. Zhang, H. Yan, P. Xiang, X. Dong, and Y. Wang, *Journal of the American Ceramic Society* **87**, 602-605
7. E. C. Subbarao, *Journal of Physics and Chemistry of Solids* **23**, 665-676 (1962).
8. R. E. Newnham, R. W. Wolfe, R. S. Horsey, F. A. Diaz-Colon, and M. I. Kay, *Materials Research Bulletin* **8**, 1183-1195 (1973).
9. R. Bechmann, *Journal of the Acoustical Society of America* **28**, 347-350
10. G. A. Smolenskii, V. A. Isupov, A. I. Afranovskaya, and N. N. Krainik, *J. Sov. Phys. Sol. Stat.* **2**, 2651-2654
11. L. EGERTON and D. M. DILLON, *JOURNAL OF THE AMERICAN CERAMIC SOCIETY* **42**, 438-442
12. F. Jona and G. Shirane, *Ferroelectric Crystals* (Pergamon Press, New York,
13. M. Kosec and D. Kolar, *Materials Research Bulletin*